

# PROCEEDINGS OF SPIE

[SPIDigitalLibrary.org/conference-proceedings-of-spie](https://spiedigitallibrary.org/conference-proceedings-of-spie)

## Broadband immersion laser ultrasonic tomography of graphite-epoxy composite

V. Zarubin, A. Bychkov, V. Simonova, E. Cherepetskaya,  
A. Karabutov

V. Zarubin, A. Bychkov, V. Simonova, E. Cherepetskaya, A. Karabutov, "Broadband immersion laser ultrasonic tomography of graphite-epoxy composite," Proc. SPIE 11210, Fourteenth School on Acousto-Optics and Applications, 1121004 (11 November 2019); doi: 10.1117/12.2540104

**SPIE.**

Event: Fourteenth School on Acousto-Optics and Applications, 2019, Torun, Poland

# Broadband immersion laser ultrasonic tomography of graphite-epoxy composite

V. Zarubin<sup>a, b</sup>, A. Bychkov<sup>a, b</sup>, V. Simonova<sup>d</sup>, E. Cherepetskaya<sup>a</sup>, and A. Karabutov<sup>a, c, d</sup>

<sup>a</sup>The National University of Science and Technology "MISIS", 4 Leninskiy prospekt, 119049 Moscow, Russia

<sup>b</sup>Faculty of Physics, Lomonosov Moscow State University, 1 Leninskiye gory, 119234 Moscow, Russia

<sup>c</sup>The International Laser Center of Lomonosov Moscow State University, 1 Leninskiye gory, 119991 Moscow, Russia

<sup>d</sup>The Institute on Laser and Information Technologies of the Russian Academy of Sciences, 1 Svyatoozerskaya St, 140700 Shatura, Moscow, Russia

## ABSTRACT

Laser ultrasonic tomography uses pulsed laser radiation for photoacoustic excitation of short probe ultrasonic pulses in a dedicated light-absorbing plate. Probe pulse propagates through immersion liquid, undergoes scattering by a surface of an object and by internal inhomogeneities. Scattered waves are recorded by a wideband multi-element acoustic array, and then used for reconstruction of the object image. A wide spectral band (0.1 - 15 MHz) of the pulse well suits a problem of inspection of carbon fiber reinforced composites, allowing visualizing of individual layers of carbon fiber, delaminations of thickness with high accuracy. In this paper, a laser ultrasonic tomography for inspection of composites is proposed. Experimental setup and results of inspection of graphite-epoxy composite sample with inclusions and defects are presented.

**Keywords:** Broadband laser ultrasound, tomography, composites, acoustic refraction

## 1. INTRODUCTION

Graphite-epoxy composites are widely used as construction materials providing improved elastic, strength properties in combination with decreased weight compared to traditionally used materials. However, the complicated technologies of production may lead to such defects, as porosity, excess or lack of binder, and cavities. The production defects can lead to more serious damage of materials during operation, e.g. lamination, cracks and further destruction of material structure.

All this leads to the increased importance of development of new methods for fast and accurate nondestructive testing and evaluation of such materials in production and in operation. The most effective of them are x-ray and ultrasonic inspection.<sup>1,2</sup> X-ray inspection provides high resolution, but has lower sensitivity and requires access to the object from several sides, which can be difficult for large objects.

Ultrasonic methods commonly use generation and detection of ultrasonic beam by the same piezoelectric transducer. However, narrow band of acoustic beams excited in such way does not allow detecting of defects with sizes from a wide range: defects of the specified size effectively scatter waves of the corresponding wavelengths. This is the reason for use of multiple transducers with different central frequencies for inspection of the same part of the composite object. Such approach decreases efficiency, speed and accuracy of nondestructive testing. On the other hand, the increase of the excitation frequency will not lead to the increase of defectoscopy resolution due to strong absorption of high-frequency ultrasound.

In this case laser ultrasonic inspection can be advantageous. It uses pulsed laser radiation to excite probe ultrasonic beams with a wide range of frequencies from hundreds of kHz to tens of MHz. Such wide spectral band allows accurate detecting of defects of different sizes and estimating of porosity of composites. So far only

---

E-mail: zarubin.vasily@gmail.com

Fourteenth School on Acousto-Optics and Applications, edited by Ireneusz Grulkowski,  
Bogumił B. J. Linde, Martí Duocastella, Proc. of SPIE Vol. 11210, 1121004  
© 2019 SPIE · CCC code: 0277-786X/19/\$21 · doi: 10.1117/12.2540104

laser ultrasonic inspection with single transducer has been applied.<sup>3</sup> In this study we present a laser ultrasonic tomographic imaging system of composites working in reflection mode. It uses pulsed laser radiation to excite short probe ultrasonic beams and acoustic multi-element array to receive scattered and reflected waves. The proposed approach combines high accuracy and high speed of operation.

## 2. EXPERIMENTAL METHOD

A sample used in the present study is a graphite-epoxy composite manufactured from graphite fibers of 5  $\mu\text{m}$  thickness, stacked unidirectionally in layers in epoxy base (Fig. 1).<sup>4</sup> This material can be treated as transversely isotropic within a good approximation for ultrasonic wavelengths longer than diameter of fibers. Hence, the composite is acoustically anisotropic. The sample has near-surface ( $\sim 2$  mm depth) metal foil insertion of  $\sim 300$   $\mu\text{m}$  thickness.

Two laser ultrasonic setups were used in the present study for imaging of the samples. The first one is UDL-2M structuroscope,<sup>5</sup> which uses pulsed laser radiation for excitation of probe ultrasonic pulses and single broadband polyvinylidene fluoride (PVDF) transducer for recording of scattered waves. The transducer is mounted on an automatized 3-axis positioning system. This setup was used to verify measurements carried out by laser ultrasonic tomographic system.

The laser ultrasonic experimental setup for tomography operates as follows.<sup>6</sup> Electromagnetic radiation of a Q-switched Nd:YAG laser (wavelength  $\lambda = 1064$  nm pulse duration  $\tau = 10$  ns, pulse repetition rate - 20 Hz) is delivered by an optical fiber to an optoacoustic generator (special light-absorbing plate) for excitation of ultrasonic pulse by means of the opto-acoustic effect. A flat-concave acoustical lens focuses the laser ultrasonic probing pulse on the sample. It passes through immersion liquid, partially reflects from the surface of the sample under inspection, and passes backwards through the same lens to be recorded by a plane piezoelectric detector array of 16 PVDF transducers (length, 20 mm; width, 1 mm; gap between transducers - 1 mm). Detector array provides effective reception of ultrasound in the frequency band of 0.1-15 MHz. The acoustic lens is introduced to make the antenna effectively focused. The system has 4-axis sample positioning system with 3 translational axes and rotational axis.

The analog electrical signals from the piezoelectric transducers after pre-amplifier are received by a high-speed multichannel data acquisition and processing system. It digitizes signals using a 50 MHz multichannel analog-to-digital converter. The system acquires digital data, averages and transfers digital data to a personal computer for further real-time data processing, which includes calculation of laser ultrasonic images and segmentation of the surface profile. A specialized software with a graphical user interface was developed to operate the experimental setup and to display images of acoustic inhomogeneities in real time (frame rate - 10 Hz). To provide the real-time mode of operation, algorithms were parallelized using NVIDIA CUDA technique of computations on graphical processing units (NVIDIA GeForce GTX 770).

The algorithms used to reconstruct images of composites are developed for imaging of isotropic samples.<sup>6</sup> Hence, taking into account the geometry and anisotropy of the sample, the algorithms allow measuring accurately sample dimensions along  $z$ -axis. The algorithm is based on the heuristic ray-tracing technique and has four stages: 1) reconstruction of a 2D laser ultrasonic tomogram using standard ltered back-projection algorithm assuming homogeneous media; 2) segmentation of the 2D surface prole of the object from the tomogram; 3) refraction-corrected re-reconstruction of the part of the tomogram corresponding to the interior of the object.

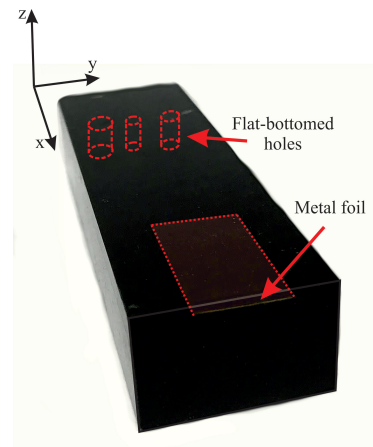


Figure 1. Graphite-epoxy composite sample of 20 mm thickness with piece of metal foil and bottom-drilled holes with diameters of 5 mm, 3 mm and 1.5 mm on the depth of 12-16 mm.

### 3. RESULTS

Fig. 2 shows comparison of images of sample cross-section in the plane  $xz$  taken by two laser ultrasonic setups. The left image Fig. 2(a) was obtained by UDL-2M scanner for 10 seconds, and the right one Fig. 2(b) was obtained for approximately 1 second by tomographic system. Fig. 2(a) is reconstructed assuming homogenous distribution of speed of sound equal to that in composite along  $z$ -axis  $\sim 3100$  m/s. Fig. 2(b) is reconstructed using refraction-corrected algorithm, which assumes homogenous distribution of speed of sound in immersion liquid  $\sim 1500$  m/s and in composite sample along  $z$ -axis  $\sim 3100$  m/s. Both images correctly show thickness of the sample (distance between reflections 1 and 5)  $\sim 20$  mm.

The bottom signal 5 in every image is formed mainly by low-frequency components (broadened line compared to line 1) of the probe wave, as higher frequencies are absorbed in the near-surface part of the sample. Reflection 3 on the images corresponds to the position of metal foil inside the sample at a depth of  $\sim 1.4$  mm. Upper red area 4 of Fig. 2(a) corresponds to the few reverberations of the probe pulse between sample surface and metal foil. Lower red area 4 and reverberation 6 correspond to a spurious reverberations of all recorded pulses (reflections from surface and metal foil) inside the acoustic path of the UDL-2M. Fig. 2(b) has the only area 4 covered by red due to longer damper of acoustic path of the tomographic system. However, this image has strong arc-like artifacts (yellow area 7), which are the features of the back-projection algorithms when a small number of receivers is used.

Both approaches allow visualizing layers of the composite (Fig. 2(c),(d)), which have thickness  $\sim 100\mu\text{m}$ . However, the visualization of layers is possible when the strong filtering of low frequencies is applied in the range 5 - 15 MHz. The low-frequency components have much higher amplitudes than high-frequency and does not allow straightly visualize layers. Images of layers Fig. 2(c)(d) were obtained with corresponding filtering of low-frequency components. The number of layers between the surface and the metal foil visualized by both setups is equal to 8, and their thickness is  $\sim 100\mu\text{m}$ . However, Fig. 2(d) shows entangled layers, what is caused by the strong back-projection arc-like artefacts.

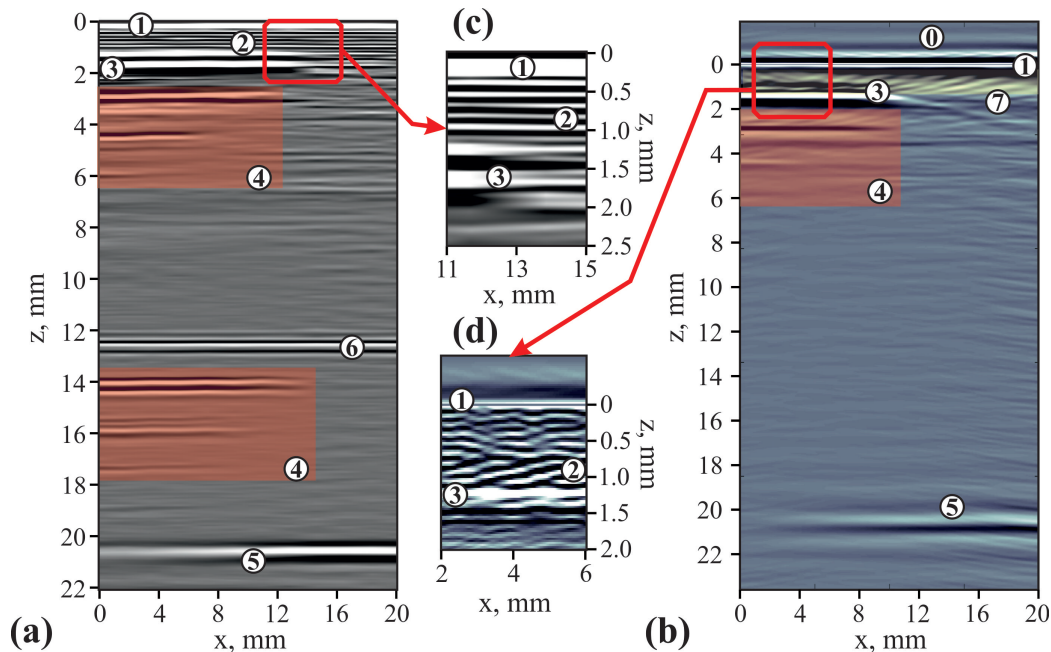


Figure 2. Comparison of laser ultrasonic images obtained by single transducer system (a), (c) and tomographic system (b), (d). (c), (d) - zoomed and high-frequency parts of images (a), (b) showing composite layers. 0 - immersion liquid; 1 - sample surface; 2 - composite layers; 3 - metal foil; 4 - reverberations; 5 - bottom signal; 6 - spurious signal; 7 - arc-like artifacts.

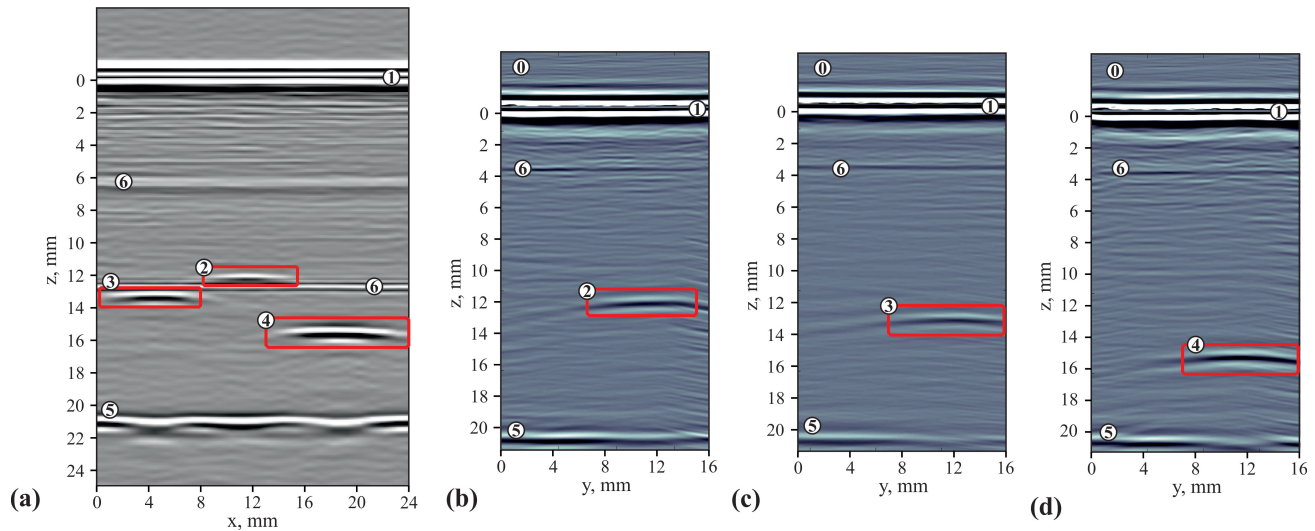


Figure 3. Images of bottom-drilled holes obtained by (a) laser ultrasonic single-transducer system and (b)-(d) and laser ultrasonic tomographic system. 0 - immersion liquid; 1 - sample surface; 2 - 1.5 mm diameter hole; 3 - 3 mm diameter hole; 4 - 5 mm diameter hole; 5 - bottom signal; 6 - spurious signal.

Fig. 3(a) shows image of the bottom-drilled holes of different sizes taken by UDL-2M scanner along  $x$ -axis. Fig. 3(b)-(d) are taken by tomographic system as a cross-sections of the sample in the cross-section by  $yz$ -plane. The positions of the holes obtained by two setups are in a good agreement.

#### 4. CONCLUSIONS

In this study the immersion laser ultrasonic tomographic system for imaging and defectoscopy composites is proposed. The system allowed visualizing of the near-surface metallic inclusion in the uniaxial graphite-epoxy composite, the bottom-drilled holes of different diameters and near-surface composite layers of  $100\ \mu\text{m}$  thickness. The system provides 10 times higher speed of operation and similar resolution comparing with single-element laser ultrasonic system UDL-2M. The proposed method benefits applications, where immersion inspection can be used, and in this case the problem of contact between transducer and object is eliminated.

#### ACKNOWLEDGMENTS

This work was supported by the Ministry of Education and Science of the Russian Federation grant K2-2019-004.

#### REFERENCES

- [1] Quan, Z., Larimore, Z., and et. al., "Microstructural characterization of additively manufactured multi-directional preforms and composites via x-ray micro-computed tomography," *Compo. Sci. Technol.* **113**, 48–60 (2016).
- [2] Nelson, L. K. and Smith, R. A., "Fibre detection and stacking sequence measurement in carbon fibre composites using radon transforms of ultrasonic data," *Composites Part A* **118**, 1–8 (2019).
- [3] Podymova, N. B. and Karabutov, A. A., "Combined effects of reinforcement fraction and porosity on ultrasonic velocity in sic particulate aluminum alloy matrix composites," *Composites: Part B* **113**, 138–143 (2017).
- [4] Karabutov, A. A., Kershtein, I. M., Pelivanov, I. M., and Podymova, N. B., "Propagation of longitudinal and shear acoustic video pulses in graphite-epoxy composites," *Acoust. J.* **45**(1), 86–91 (1999).
- [5] Karabutov, A., Devichensky, A., Ivochkin, A., Lyamshev, M., Pelivanov, I., Rothatgi, U., Solomatin, V., and Subudhi, M., "Laser ultrasonic diagnostics of residual stress," *Ultrason.* **48**(6-7), 631–635 (2008).

- [6] Zarubin, V., Bychkov, A., Zhigarkov, V., Karabutov, A., and Cherepetskaya, E., “Model-based measurement of internal geometry of solid parts with sub-psf accuracy using laser-ultrasonic imaging,” *NDT and E Int.* **105**, 56–63 (2019).